PAPER • OPEN ACCESS

Effect of carbon content, deformation and annealing on the structure and properties of interstitial TRIP high-entropy alloys

To cite this article: D G Shaysultanov *et al* 2021 *IOP Conf. Ser.: Mater. Sci. Eng.* **1014** 012052

Effect of carbon content, deformation and annealing on the structure and properties of interstitial TRIP high-entropy alloys

D G Shaysultanov*, K Sh Raimov and N D Stepanov

Belgorod State National Research University, Pobeda, 85, Belgorod, 308015, Russia

*Corresponding author: shaysultanov@bsu.edu.ru

Abstract. In this work, the effect of carbon content on the structure and mechanical properties of $Fe_{(50-x)}Mn_{30}Co_{10}Cr_{10}C_x$ (x=0; 0.5; 1.0 at.%) interstitial high entropy alloys was studied. In the as-cast condition, the alloys were composed of the face centred cubic (fcc) and hexagonal close packed (hcp) phases; the amount of the hcp phase decreased from 46% to 20% as the carbon concentration increased from 0 to 1 at.%. The carbon content had a limited effect on the strength of the alloys, yet the ductility was enhanced significantly as the result of interstitial alloying. Furthermore, $Fe_{49}Mn_{30}Co_{10}Cr_{10}C_1$ alloy was cold rolled to a reduction of 56% reduction and annealed at 700-900˚C for 1 hour. After cold working, the alloy has attained almost fully the hcp structure. Annealing resulted in (i) transformation of the deformation-induced hcp phase into fcc; (ii) development of recovery and recrystallization; (iii) precipitation of Cr-rich $M_{23}C_6$ carbides. The cold-rolled alloy was very strong but brittle; annealing resulted in softening and increase of the ductility. The relationships between the chemical composition, structure and mechanical properties of the alloys are briefly discussed.

1. Introduction

The so-called high-entropy alloys (HEAs) have recently emerged as promising materials with unprecedent mechanical characteristics, for example, a combination of strength and ductility [1]. Excellent properties of the alloys often come from the synergy of different deformation mechanisms. For instance, Z. Li et al. introduced $Fe_{50}Mn_{30}Co_{10}Cr_{10}$ (in at.%) alloy composed from two (face centered cubic, fcc and hexagonal close packed, hcp) phases, exhibiting transformation-induced plasticity (TRIP) effect [2]. The mechanical properties of HEAs can be significantly enhanced by the addition of interstitial elements like carbon or nitrogen [3,4], as was demonstrated in $Fe_{49.5}Mn_{30}Co_{10}Cr_{10}C_{0.5}$ alloy [5]. In this case, the alloy additionally benefited from interstitial solid solution hardening and precipitate (carbide) hardening. However, many aspects of the effect of carbon on the structure and properties of interstitial TRIP HEAs remain unclear. In addition, it is not completely clear how the structure and properties of such alloys evolve during thermomechanical processing [6]. Therefore, in this work, we (i) have examined the effect of carbon content (0-1 at.%) on the structure of the as-cast $Fe_{50}Mn_{30}Co_{10}Cr_{10}$-based alloys and (ii) studied the effect of thermomechanical processing on the structure and properties of the alloy with 1 at.% C.

IOP Conf. Series: Materials Science and Engineering 1014 (2021) 012052 doi:10.1088/1757-899X/1014/1/012052

2. Materials and methods

A series of the $Fe_{(50-x)}Mn_{30}Co_{10}Cr_{10}C_x$ (x=0; 0.5; 1.0 at.%) alloys were prepared by vacuum arc melting technique. High-purity (≥99.9 wt.%) elements were used as starting materials. The alloys were examined in the as-cast condition. In addition, the alloy with x=1 at.% C ($Fe_{49}Mn_{30}Co_{10}Cr_{10}C_1$) was subjected to cold rolling with a reduction of 56% and subsequent annealing at 700-900˚C for 1 hour.

A scanning electron microscope with an electron backscattered diffraction (EBSD) attachment was primarily used for the microstructure characterization. Careful mechanical polishing on grinding papers with continuously decreasing grain size and final polishing with OP-S suspension was performed to prepare the specimens for microstructure characterization. In addition, transmission electron microscopy (TEM) method was used to get better understanding of the structure of the alloys in some conditions.

The mechanical properties of the alloys were accessed by tensile tests at room temperature. Dog-bone specimens with the gauge dimensions of 12×3×1.5 mm^3 were pulled to fracture with the initial strain rate of 10^{-3} s^{-1}.

3. Results and Discussion

The as-cast microstructures of the $Fe_{(50-x)}Mn_{30}Co_{10}Cr_{10}C_x$ (x=0; 0.5; 1.0 at.%) alloys are shown in figure 1. All alloys had a similar coarse grain size of 300-400 μm (not shown). Inside the grains, a dual-phase structure, composed of fcc and hcp phases, was observed. The addition of carbon has resulted in a gradual decrease in the fraction of the hcp phase: from 46% in the x=0 alloy to 36% in the x=0.5 alloy and, finally, to 20% on the x=1.0 alloy. The decrease in the hcp fraction is most likely associated with an increase of the stacking fault energy of the alloy due to carbon alloying. Also, the morphology of the hcp particles was affected by carbon alloying. In the carbon-free alloy, the particles had regular, plate-like shape with sharp straight boundaries. An increase in the carbon concentration resulted in more equiaxed particles with irregular shape and curved boundaries. Note that the TEM studies (the results are not shown) did not reveal the presence of any other phases than fcc and hcp.

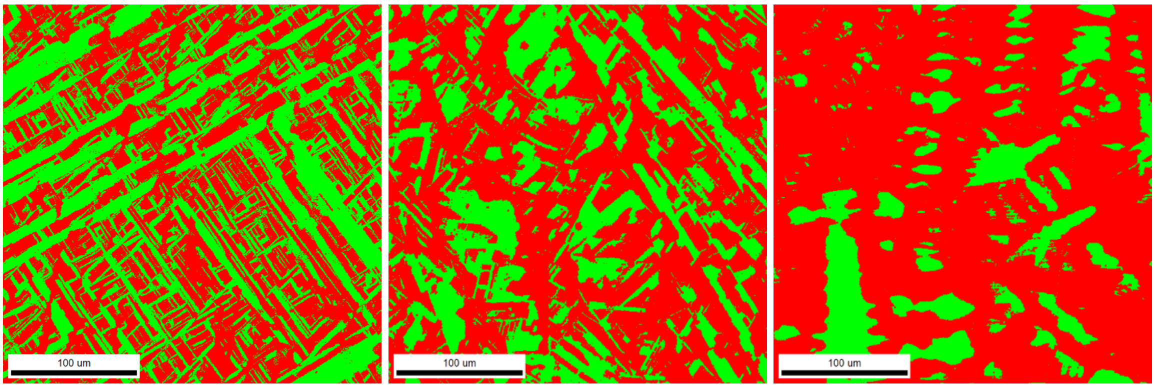

a b c

Figure 1. EBSD phase maps of the $Fe_{(50-x)}Mn_{30}Co_{10}Cr_{10}C_x$ alloys: a - x=0 at.%; b – x=0.5 at.%; c – x=1.0 at.%. The hcp phase is shown in green color and the fcc phase – in red color.

The x=1 ($Fe_{49}Mn_{30}Co_{10}Cr_{10}C_1$) alloy was further subjected to cold rolling and subsequent annealing at 700-900˚C (figure 2). After cold working, the alloy had mostly hcp structure (figure 2a), which was a product of the deformation-induced martensitic transformation. The fraction of the fcc phase was only 13%; fcc particles had a characteristic plate-like morphology. Note the presence of black areas on the EBSD phase map; they indicate the low quality of the obtained Kikuchi patterns and the high density of defects in the alloy after rolling. Annealing at 700˚C results in drastic changes in the microstructure (figure 2b, c). First, the deformation-induced hcp phase was mostly converted to the fcc phase; the fraction of the hcp phase was 15%. Partial recrystallization also occurred; the fraction and the size of the recrystallized grains were 62% and 1.8 μm, respectively. In the uncrystallized areas, the recovery took place as evidenced from the absence of black areas with low image quality. A further increase in the annealing temperature to 900˚C resulted in the formation of a fully recrystallized microstructure with a mean grain size of 7.0 µm (figure 2d, e). The fraction of the hcp phase decreased further to 5%. In addition, TEM studies revealed the presence of Cr-rich $M_{23}C_6$ type carbides in the fcc matrix (figure 2f). The fraction and the size of the carbides were 4% and 140 nm, respectively. Note that similar carbides were detected already after annealing to 700˚C (not shown).

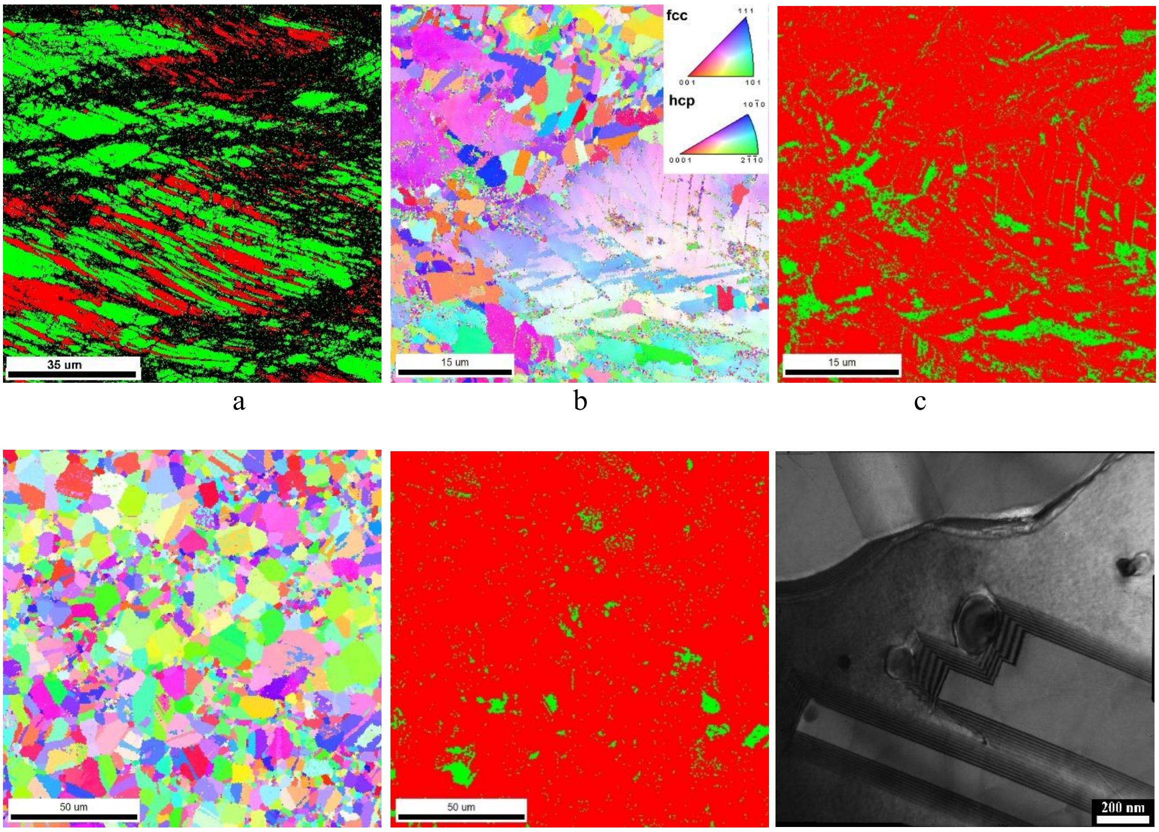

d e f

Figure 2. Microstructure of the $Fe_{49}Mn_{30}Co_{10}Cr_{10}C_1$ alloy after thermomechanical processing: a – cold rolling to a reduction of 56%; b, c – subsequent annealing at 700˚C; d, e, f – subsequent annealing at 900˚C. a, c, e – EBSD phase maps (color coding is the same as in figure 1); b, d – EBSD IPF maps; f – TEM bright-field image.

The effect of chemical composition and processing on the mechanical properties of the program $Fe_{(50-x)}Mn_{30}Co_{10}Cr_{10}C_x$ alloys was evaluated using tensile testing (figure 3). The carbon content had a strong and not readily anticipated effect on the mechanical properties of the as-cast alloys. The $Fe_{50}Mn_{30}Co_{10}Cr_{10}$ and $Fe_{49}Mn_{30}Co_{10}Cr_{10}C_1$ alloy had rather close strength – yield strength of 245 MPa and 240 MPa, respectively, and ultimate tensile strength of 705 MPa and 680 MPa (figure 3a). However, the carbon-doped alloy had more than 2 times better ductility – the respective values of uniform elongation were 38% and 86%, respectively. Such a huge difference in ductility can be potentially attributed to a higher fraction of the softer fcc phase (figure 1) that can transform to a harder hcp phase during plastic deformation and thus provide effective strain hardening, i.e. the enhanced TRIP effect. Yet, this assumption is contrary to the recent results on similar $Fe_{50}Mn_{30}Co_{10}Cr_{10}$ alloy [6]. Thus, additional work is required to elucidate the reasons of improved ductility of the carbon-doped alloys.

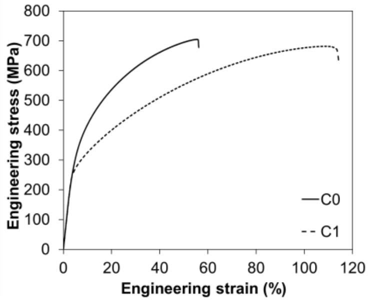

a

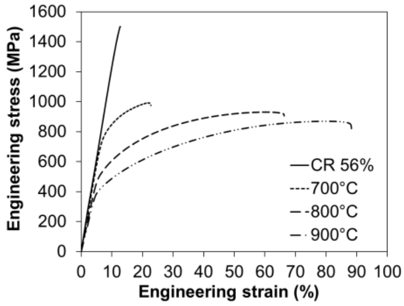

b

Figure 3. Stress-strain curves obtained during tensile testing of: a – as-cast $Fe_{(50-x)}Mn_{30}Co_{10}Cr_{10}C_x$ (x=0 and x=1) alloys; b - $Fe_{49}Mn_{30}Co_{10}Cr_{10}C_1$ after thermomechanical processing.

Thermomechanical processing had a more anticipated effect on the mechanical properties of the $Fe_{49}Mn_{30}Co_{10}Cr_{10}C_1$ alloy (figure 3b). The cold-worked alloy had high strength (yield strength of 1415 MPa), but very limited ductility (0.5%), probably due to the mostly hcp structure (figure 2a). Annealing at 700˚C resulted in considerable softening (yield strength of 680) due to the transition of hcp to fcc (figure 2c), but the ductility remained rather low (10%) because of the partially recrystallized microstructure. Excellent ductility was obtained in the fully recrystallized alloy after annealing at 900˚C (68%). The yield strength of the annealed alloy was 370 MPa. The obtained results clearly suggest typical strength-ductility trade-off in the $Fe_{49}Mn_{30}Co_{10}Cr_{10}C_1$ alloy.

4. Conclusions

1) The increase in the carbon percentage from 0 to 1 at.% resulted in a decrease in the hcp phase fraction from 46% to 20% in the as-cast $Fe_{(50-x)}Mn_{30}Co_{10}Cr_{10}C_x$ alloys. The strength of the alloys showed some decrease with carbon addition, however, the ductility increased substantially.
2) After cold rolling, the $Fe_{49}Mn_{30}Co_{10}Cr_{10}C_1$ alloy had almost fully the hcp structure. Annealing at 700-900˚C resulted in (i) transformation of deformation-induced hcp phase into fcc; (ii) development of recovery and recrystallization; (iii) precipitation of Cr-rich $M_{23}C_6$ carbides. The cold-rolled alloy was very strong but brittle; annealing resulted in softening and an increase of the ductility.

Acknowledgements

The authors gracefully acknowledge the financial support from the Russian Science Foundation, grant № 20-79-10093.

References

[1] Miracle D B and Senkov O N 2017 A critical review of high entropy alloys and related concepts *Acta Mater.* **122** 448–511
[2] Li Z, Pradeep K G, Deng Y, Raabe D and Tasan C C 2016 Metastable high-entropy dual-phase alloys overcome the strength–ductility trade-off *Nature* **534**
[3] Klimova M V, Semenyuk A O, Shaysultanov D G, Salishchev G A, Zherebtsov S V and Stepanov N D 2019 Effect of carbon on cryogenic tensile behavior of CoCrFeMnNi-type high entropy alloys *J. Alloys Compd.* **811** 152000
[4] Klimova M, Shaysultanov D, Semenyuk A, Zherebtsov S, Salishchev G and Stepanov N 2020 Effect of nitrogen on mechanical properties of CoCrFeMnNi high entropy alloy at room and cryogenic temperatures *J. Alloys Compd.* 156633
[5] Li Z, Tasan C C, Springer H, Gault B and Raabe D 2017 Interstitial atoms enable joint twinning and transformation induced plasticity in strong and ductile high-entropy alloys *Sci. Rep.* **7** 40704
[6] Li Z, Tasan C C, Pradeep K G and Raabe D 2017 A TRIP-assisted dual-phase high-entropy alloy: Grain size and phase fraction effects on deformation behavior *Acta Mater.* **131** 323–35